Arpeeta Sharma,[1,2,3] Stephanie Sellers,[1,2] Nada Stefanovic,[3] Cleo Leung,[1,2] Sih Min Tan,[3] Olivier Huet,[3] David J. Granville,[2,4] Mark E. Cooper,[3,5] Judy B. de Haan,[3,5] and Pascal Bernatchez[1,2]

Direct Endothelial Nitric Oxide Synthase Activation Provides Atheroprotection in Diabetes-Accelerated Atherosclerosis

Diabetes 2015;64:3937–3950 | DOI: 10.2337/db15-0472

Patients with diabetes have an increased risk of developing atherosclerosis. Endothelial dysfunction, characterized by the lowered bioavailability of endothelial NO synthase (eNOS)–derived NO, is a critical inducer of atherosclerosis. However, the protective aspect of eNOS in diabetes-associated atherosclerosis remains controversial, a likely consequence of its capacity to release both protective NO or deleterious oxygen radicals in normal and disease settings, respectively. Harnessing the atheroprotective activity of eNOS in diabetic settings remains elusive, in part due to the lack of endogenous eNOS-specific NO release activators. We have recently shown in vitro that eNOS-derived NO release can be increased by blocking its binding to Caveolin-1, the main coat protein of caveolae, using a highly specific peptide, CavNOxin. However, whether targeting eNOS using this peptide can attenuate diabetes-associated atherosclerosis is unknown. In this study, we show that CavNOxin can attenuate atherosclerotic burden by ~84% in vivo. In contrast, mice lacking eNOS show resistance to CavNOxin treatment, indicating eNOS specificity. Mechanistically, CavNOxin lowered oxidative stress markers, inhibited the expression of proatherogenic mediators, and blocked leukocyte-endothelial interactions. These data are the first to show that endogenous eNOS activation can provide atheroprotection in diabetes and suggest that CavNOxin is a viable strategy for the development of antiatherosclerotic compounds.

Diabetes is widely regarded as an independent risk factor for the development of cardiovascular diseases, with ~80% of cardiovascular mortality and morbidity being linked to macrovascular complications, such as atherosclerosis (1–3). The increased risk of development of vascular complications in individuals with type 1 (T1D) or type 2 diabetes (T2D) occurs despite intensive glycemic control, stressing the need for novel approaches to lessen the burden of diabetes-mediated macrovascular injury (4).

The vascular endothelium plays a crucial role in diabetes-associated atherosclerosis through the regulation of vessel permeability, inflammation, coordination of leukocyte trafficking, and thrombosis (1,5). Indeed, the function of the vascular endothelium is significantly impaired during diabetes, a phenomena termed endothelial dysfunction and characterized by the reduced bioavailability of an important endothelial cell mediator, nitric oxide (NO). Such chronic attenuation of endothelial-derived NO release promotes platelet and leukocyte activation and adhesion, compromises endothelial cell barrier integrity, and causes the upregulation of proinflammatory genes (6–8). Moreover, reduced NO-dependent vasodilation and increased leukocyte adhesion to the endothelium, both of which are hallmarks of endothelial dysfunction, have been observed in patients with diabetes and diabetic animal models (9–12). Similarly, in cultured endothelial cells exposed to high glucose, lowered endothelial NO synthase (eNOS)–derived NO release was observed (13–15). In addition, endothelial dysfunction, diabetes, and atherosclerosis are linked to a heightened state of oxidative

[1]Department of Anesthesiology, Pharmacology and Therapeutics, University of British Columbia, Vancouver, British Columbia, Canada
[2]Centre for Heart Lung Innovation, St. Paul's Hospital, University of British Columbia, Vancouver, British Columbia, Canada
[3]Baker IDI Heart and Diabetes Institute, Diabetic Complications Division, Melbourne, Victoria, Australia
[4]Department of Pathology and Laboratory Medicine, University of British Columbia, Vancouver, British Columbia, Canada
[5]Department of Immunology, Monash University, Melbourne, Victoria, Australia

Corresponding authors: Judy B. de Haan, judy.dehaan@bakeridi.edu.au, and Pascal Bernatchez, pascal.bernatchez@ubc.ca.

Received 7 April 2015 and accepted 20 June 2015.

This article contains Supplementary Data online at http://diabetes.diabetesjournals.org/lookup/suppl/doi:10.2337/db15-0472/-/DC1.

J.B.d.H. and P.B. made equal contributions as senior authors.

See accompanying article, p. 3645.

stress and its main mediator, superoxide anion. Superoxide can scavenge free NO to form peroxynitrite, another potent reactive oxygen species (ROS), which significantly contributes to lower NO bioavailability.

Atheroprotective NO is released by the endothelium via the constitutively expressed eNOS, the dimeric NOS isoform that is activated by hemodynamic factors and agonists. Genetic deletion or pharmacological inhibition of eNOS in preclinical models increases atherosclerotic burden significantly, providing clear evidence of the antiatherogenic role of eNOS-derived NO (16,17). However, eNOS overexpression in mice also accelerates atherosclerosis, a likely consequence of uncoupling of the enzyme to its monomeric state, resulting in the production of deleterious superoxide instead (18). Hence, proper eNOS regulation is critical to its atheroprotective function (19). eNOS-derived NO is regulated by phosphorylation of the enzyme and availability of its substrates (L-arginine) and cofactors (BH4). Furthermore, optimal NO release requires eNOS trafficking to caveolae, which are lipid-enriched organelles at the plasma membrane known to maintain spatial organization of signaling complexes and participate in signal transduction events (20). Within caveolae, basal eNOS activity is maintained under tight inhibitory control by Caveolin-1 (Cav-1), the main coat protein of caveolae, through a direct protein–protein interaction between the scaffolding domain (amino acids 82–101) of Cav-1 and eNOS (21–24). Upon agonist (vascular endothelial growth factor acetylcholine)–induced increases in intracellular Ca^{2+}, eNOS recruits calmodulin and HSP90, which facilitates the dissociation of Cav-1 from eNOS, resulting in the stimulus-response coupling of eNOS leading to the production of NO (20). We have shown that threonine 90,91 and especially phenylalanine 92 (T90,91,F92) in the Cav-1 scaffolding domain are responsible for inhibiting eNOS-derived NO release (21). Furthermore, this inhibitory domain is distinct from the binding domain because a mutated protein, F92A Cav-1, binds eNOS but fails to inhibit its activity (25,26). However, when coexpressed in endothelial cells expressing eNOS and inhibitory Cav-1, F92A Cav-1 caused an unexpected but robust increase in unstimulated eNOS-derived NO release (25). These observations revealed the strong inhibitory action of Cav-1 on eNOS and strengthened the concept of eNOS/Cav-1 antagonism: preventing eNOS binding to inhibitory Cav-1 results in increased basal NO release. Indeed, a cell-permeable, Cav-1–derived peptide with T90,91,F92 substituted to alanines, known as CavNOxin, can increase eNOS activity in reconstituted and endothelial cells (21,25) and reduce vascular tone ex vivo, an effect that was completely abolished in eNOS and Cav-1 knockout (KO) mice (25). These highly eNOS and Cav-1–specific biological functions of CavNOxin are the first to show increased NO release through regulated eNOS/Cav-1 interactions while preserving Cav-1–dependent biological activities such as caveolae formation (25).

In this study, we have investigated whether improving NO release through the use of CavNOxin could attenuate atherosclerosis in hyperglycemic settings. We report that treatment of diabetic mice with CavNOxin normalizes a range of oxidative stress and inflammatory markers and attenuates diabetes-induced atherosclerosis by up to 84%, whereas eNOS gene inactivation renders diabetic animals resistant to CavNOxin treatment. Most importantly, our data suggest that exogenous agents can directly and specifically trigger the protective function of eNOS, indicating that this interaction should be considered a direct pharmacological target to lessen the burden of diabetic end-organ injury such as atherosclerosis.

RESEARCH DESIGN AND METHODS

Animals

Apolipoprotein E (ApoE) KO mice were purchased from the Animal Resource Centre (Western Australia) and The Jackson Laboratory (Bar Harbor, ME) and housed at the Alfred Medical Research and Education Precinct animal facility and the genetically engineered model facility at the University of British Columbia James Hogg Research Centre, respectively. All experiments were approved by the respective animal care committees. To generate eNOS/ApoE double KO (dKO) mice, eNOS KO mice were purchased from The Jackson Laboratory and cesarean rederived used to generate eNOS KO mice on a pure C57BL/6 background. eNOS KO mice were crossed to ApoE KO mice, and resulting mice heterozygous for both eNOS and ApoE were then crossed with ApoE KO mice. Finally, littermates that were ApoE KO/eNOS heterozygous were bred together to give age-matched littermates that were ApoE KO and eNOS wild-type, eNOS heterozygous, or eNOS KO.

Experimental Design

To generate an insulin-deficient model reflecting T1D, 8-week-old male ApoE KO mice were rendered diabetic by intraperitoneal injections of streptozotocin (STZ; 100 mg/kg/day) or citrate buffer (nondiabetic [ND] controls) on 2 consecutive days. After 2 weeks, mice were randomized and injected intraperitoneally every 3 days with sterile water, vehicle peptide (Antennapedia, dissolved in 1% DMSO in sterile water, the same molar dose as CavNOxin), or CavNOxin at 2.5 and 5.0 mg/kg (dissolved in 1% DMSO in sterile water) for 14 weeks. Previous studies by our group demonstrated that this length of time allows for the development of robust atherosclerotic plaque within the vessel walls and aortic sinus in diabetic ApoE KO mice (27). Nonfasted blood glucose readings were measured every week to confirm that mice were diabetic throughout the study.

To generate an insulin-resistant model reflecting T2D, 8-week-old male ApoE KO mice and eNOS/ApoE dKO mice were fed a Western diet (WD) containing 22% fat and 0.15% cholesterol (Specialty feeds, SF00–219 or Harlan Teklad TD88137) ad libitum for 12 weeks (28). ApoE KO mice fed a WD exhibit a metabolic phenotype consistent with T2D, which includes elevated insulin and

glucose levels as compared with standard chow–fed mice (28–30). During the 12-week time period, mice were injected intraperitoneally every 3 days with either vehicle peptide or CavNOxin (2.5 mg/kg). A control group of male ApoE KO mice were fed standard chow diet and subjected to the same injection regimen as the WD-fed ApoE KO mice.

Atherosclerotic Lesion Analysis

At the study end point, mice were killed, and atherosclerotic lesions were assessed as described previously using the en face method after Sudan-IV staining to assess lesions within three regions of the aorta (31,32). Lesions were also determined in the heart sinus after staining with Oil Red O as described previously (31,32). For en face analysis, lesions are expressed as the percent plaque detected within a particular region, while for the aortic sinus, lesion size (μm^2) was determined from the average of five cross sections, and the results of each group are expressed as lesion size (μm^2) $\pm$ SEM.

Plasma and Urine Analysis

One week prior to termination, mice were kept in metabolic cages for a period of 24 h for the collection of urine. Urinary 8-isoprostanes was determined as a marker of oxidative stress as per the manufacturer's instructions (Caymen Chemical). At termination, animals were fasted for 12 h, and following anesthesia, blood (0.8–1 mL) was collected in heparin and immediately spun down at 4,000 rpm for 10 min to separate out plasma for analytical purposes. Plasma NO was determined using a total NO detection kit based on the principles of the Griess reaction as per the manufacturer's instructions (Enzo Life Sciences). Derivatives of reactive oxygen metabolites (dROMs) were measured in plasma as an indication of oxidative stress using the FRAS-4 system as described previously (33). Plasma glucose, cholesterol, HDL, triglycerides, and insulin were measured using commercially available enzymatic kits, and LDL was determined using the Friedewald calculation.

Quantitative RT-PCR Analysis

In another cohort of mice, aortas were snap frozen in TRIzol and total RNA was extracted after homogenization of the tissue. DNAse-free RNA and cDNA synthesis was performed as described previously (31). Probes and primers were purchased from Applied Biosystems (Foster City, CA). Gene expression of eNOS, vascular cell adhesion molecule-1 (VCAM-1), intracellular adhesion molecule-1, MCP-1, and nuclear factor-κB subunit p65 was analyzed by quantitative RT-PCR (qRT-PCR) as described previously (27).

Immunohistochemistry

Aortic paraffin sections were stained for nitrotyrosine (NT) (a marker of peroxynitrite-induced damage) and 4-HNE (a lipid peroxidation marker), while frozen aortic sections were stained for VCAM-1. In brief, paraffin sections were dewaxed, frozen aortic sections were fixed with cold acetone, and endogenous peroxidases were inactivated with 3% H_2O_2 in Tris-buffered saline. Sections were incubated with a protein blocking agent and a biotin-avidin blocking kit (Vector Laboratories). For 4-HNE staining, the Mouse On Mouse kit (M.O.M Kit; Vector Laboratories) was used in addition to localize mouse antibodies on mouse tissues. Aortic sections were then incubated with the respective primary antibody (VCAM-1: 1:100; 4-HNE: 1:100; and NT: 1:75) overnight at 4°C. Secondary antibody, biotinylated anti-rabbit immunoglobulin 1:100 (Dako), or biotinylated antirat immunoglobulin (1:200; Vector Laboratories) was then added for 30 min, followed by horseradish peroxidase–conjugated streptavidin, diluted 1:500 (Dako), and incubated for 30 min in 3,3′-diaminobenzidine tetrahydrochloride (Sigma-Aldrich) with hematoxylin counterstain. Images were visualized under light microscopy and quantitated using Image Pro Plus. On average, three to five sections were assessed per mouse, and seven to nine mice were analyzed per group.

In Vitro Experiments in Human Aortic Endothelial Cells

Human aortic endothelial cells (HAECs) (Cell Application, San Diego, CA; passage 4 to 8) were maintained in endothelial cell media (EGM-2 bullet kit; Lonza) and seeded into experimental six-well culture dishes that were precoated with fibrinogen (100 μg/mL). At 90% confluency, HAECs were serum starved and treated with either vehicle or CavNOxin peptide (5 μmol) for 6 h. This concentration and time point have previously been demonstrated by us to significantly increase NO release in endothelial cells and decrease association of endogenous Cav-1 to eNOS (25). In a separate experiment, HAECs were grown in low-glucose (5 mmol) and high-glucose (30 mmol) media for 3 days prior to peptide treatment.

Evaluation of Monocyte/Leukocyte–Endothelial Interactions In Vitro and Ex Vivo

Monocyte–endothelial interactions were determined by performing in vitro static cell adhesion assays. Briefly, human monocytic THP-1 cells were labeled with the CellVue Burgundy fluorescent labeling kit (Affymetrix) as per the manufacturer's instructions and incubated with treated HAECs (as described above) for 20 min at 37°C. Thereafter, HAECs were washed twice with PBS and fixed with 10% neutral buffered formalin, and plates were scanned using an Odyssey infra-red scanner and quantified.

Leukocyte–endothelial interactions were determined ex vivo by performing dynamic flow adhesion assays as described previously (34). Briefly, aortas from ND and diabetic ApoE KO mice were incubated with vehicle or CavNOxin peptide (10 μmol; 12 h) in the presence or absence of tumor necrosis factor-α (TNF-α) (5 ng/mL; 4 h), previously demonstrated by us to significantly reduce phenylephrine-induced contraction in isolated aortas (25). Vessels were then carefully mounted on each end of a cannula in a vessel chamber containing prewarmed Krebs buffer. Whole human blood (5 mL/vessel)

was labeled with VybrantDil (1:1,000, 10 min) and then perfused through the vessel at a rate of 100 μL/min. Labeled leukocyte interaction was visualized and quantified using a fluorescence microscope. Readings were taken at two fields along the perfused vessel for 10 s at the 5-, 10-, and 15-min time points.

Measurement of Superoxide in Aortas

Superoxide content was measured using dihydroethidium (DHE; 10 μmol/L) staining on frozen aortic sections. In brief, serial sections of flash-frozen aorta were cryosectioned at 10 μm and mounted onto slides (Menzel-Glaser SuperFrost Plus). For each aorta, DHE staining was performed in the presence or absence of 1 mmol tempol (Fluka), a superoxide dismutase mimetic, enabling the measurement of superoxide-specific DHE using a Zeiss 510 Meta confocal microscope equipped with a krypton/argon laser (excitation 488 and emission 543 nm). The intensity of the fluorescence was quantified, and superoxide-specific DHE staining equalled percent intensity of DHE stain minus percent intensity of DHE stain in the presence of tempol.

Vascular Reactivity Assays

WD-fed ApoE-KO mice were treated for 28 days with CavNOxin or vehicle peptides. Following that, the thoracic aorta was dissected out and cut into 4-mm-long segments. The rings were suspended by two tungsten wires mounted in a vessel myograph system (Danish Myotechnologies, Aarhus, Denmark) in oxygenated Krebs buffer at 37°C as published (25). To study NOS specificity of these vasoconstrictor responses, the rings were preconstricted with a submaximal concentration of phenylephrine (PE), and L-NAME (100 μmol) was injected at the plateau of the PE-induced contraction.

Data and Statistical Analysis

All data are presented as mean ± SEM and considered as statistically significant at $P < 0.05$ by one-way ANOVA followed by Newman-Keuls post hoc test. For the leukocyte–endothelial interaction ex vivo assay, a two-way ANOVA followed by a Bonferroni post hoc test was performed. For VCAM-1, DHE, 4-HNE, and NT immunohistochemical staining, data are normalized to the ND control group for the ApoE KO mice with STZ-induced diabetes and WD + vehicle group for the WD-fed ApoE KO mice.

RESULTS

CavNOxin Does Not Affect Metabolic Parameters in Mice With STZ-Induced Diabetes and in WD-Fed ApoE KO Mice

Body weight, blood glucose, and metabolic parameters of mice with STZ-induced diabetes and WD-fed ApoE KO mice are shown in Tables 1 and 2, respectively. As expected, mice with STZ-induced diabetes and WD-fed ApoE KO mice exhibited elevated fasting glucose, triglycerides, and cholesterol levels as compared with ND and standard chow–fed ApoE KO mice, respectively. The metabolic phenotypes of these mice were similar to T1D and T2D (29). Most importantly, treatment with either CavNOxin (2.5 or 5 mg/kg) or vehicle peptide did not alter glucose or lipid parameters in either model. As expected, mice with STZ-induced diabetes had an ~65% decrease in plasma insulin levels as compared with ND ApoE KO mice, with no effect in CavNOxin-treated mice (Table 1). ApoE KO mice fed a WD showed a trend toward elevated blood pressure, whereas STZ induction had no effect on basal blood pressure levels (Supplementary Fig. 4). Blood pressure was unaffected by CavNOxin treatment in both models.

CavNOxin Protects Against STZ- and WD-Induced Atherosclerosis

STZ-induced ApoE KO mice displayed a significant 9.2-fold increase in total plaque area as compared with ND ApoE KO mice (Fig. 1*A* and representative images in Supplementary Fig. 1), with increased plaque burden observed in the arch, thoracic, and abdominal areas (9.2-, 9.2-, and

Table 1—Body weight, blood glucose, glycated Hb, triglycerides, cholesterol, HDL, non-HDL cholesterol, LH ratio, and plasma insulin (ng/mL) were determined after 10 weeks of diabetes in the presence or absence of CavNOxin treatment in STZ-induced ApoE KO mice

Parameter	ND	Diabetic	Diabetic + vehicle	Diabetic + CavNOxin (2.5 mg/kg)	Diabetic + CavNOxin (5 mg/kg)
Body weight (g)	28.5 ± 0.5	25.1 ± 1.0*	24.8 ± 0.5*	27.3 ± 0.7	26.8 ± 1.4
Blood glucose (mmol/L)	8.7 ± 0.4	24.9 ± 1.8***	28.8 ± 2.7***	25.3 ± 2.4***	23.5 ± 1.1***
Glycated Hb	3.6 ± 0.1	10.5 ± 0.7***	10.4 ± 0.5***	11.1 ± 0.7***	10.5 ± 1.8***
Cholesterol	9.0 ± 0.3	18.9 ± 1.5***	22.3 ± 1.2***	18.7 ± 1.4***	17.6 ± 2.3***
Triglycerides	1.4 ± 0.1	3.5 ± 0.2**	3.9 ± 0.5**	2.9 ± 0.6*	3.4 ± 1.1*
HDL	2.0 ± 1.1	3.7 ± 0.4***	4.3 ± 0.3***	3.6 ± 0.3**	3.2 ± 0.4*
LDL	6.4 ± 0.3	13.4 ± 1.1***	16.6 ± 0.8***	13.8 ± 1.0***	12.9 ± 1.6***
LH ratio	3.2 ± 0.1	3.6 ± 0.2*	4.0 ± 0.1***	3.9 ± 0.2**	4.1 ± 0.2**
Insulin (ng/mL)	0.37 ± 0.1	0.12 ± 0.03*	0.15 ± 0.03*	0.12 ± 0.02*	0.12 ± 0.02*

All results are expressed as mean ± SEM. n = 5–10/group. Hb, hemoglobin; LH, LDL/HDL ratio. *$P < 0.05$, **$P < 0.01$, ***$P < 0.001$ vs. ND mice.

Table 2—Body weight, blood glucose, triglycerides, cholesterol, HDL, non-HDL cholesterol, and LH ratio were determined after 12 weeks of standard chow or WD in the presence or absence of CavNOxin treatment

Parameter	Chow + vehicle	Chow + CavNOxin	WD + vehicle	WD + CavNOxin
Body weight (g)	28.0 ± 1.6	30.8 ± 0.8	28.8 ± 1.5	29.4 ± 1.7
Blood glucose (mmol/L)	5.2 ± 0.3	4.7 ± 0.2	9.6 ± 0.6**	10.3 ± 0.9***
TGs (mmol/L)	1.6 ± 0.2	1.0 ± 0.2	2.8 ± 0.2*	2.6 ± 0.3*
Cholesterol (mmol/L)	7.9 ± 0.5	9.3 ± 0.6	24.2 ± 1.1***	24.5 ± 1.4***
HDL cholesterol (mmol/L)	1.5 ± 0.1	2.1 ± 0.1	4.9 ± 0.2***	4.6 ± 0.2***
Non-HDL cholesterol (mmol/L)	5.7 ± 0.3	6.8 ± 0.4	18.0 ± 0.8***	18.7 ± 1.1***
LH ratio (mmol/L)	4.0 ± 0.1	3.2 ± 0.1	3.7 ± 0.1*	4.0 ± 0.1##

All results are expressed as mean ± SEM. n = 10/group. LH, LDL/HDL ratio; TG, triglyceride. *$P < 0.05$, **$P < 0.01$, ***$P < 0.001$ vs. chow + vehicle group; ##$P < 0.01$ vs. WD + vehicle group.

7.5-fold increase, respectively) (Fig. 1*B–D*). Treatment with CavNOxin at 5 mg/kg attenuated total aortic plaque by 70% (Fig. 1*A–D*) (arch plaque area reduced by 80%, thoracic plaque area reduced by 84%), although abdominal aorta plaque reduction was not significant. A lower dose of CavNOxin (2.5 mg/kg) reduced total plaque burden by 56% (Fig. 1*A*), reflecting dose dependency. In STZ-induced ApoE KO mice, aortic sinus lesion area increased by 2.4-fold as compared with ND mice (Fig. 1*E*), which was decreased by 81% after CavNOxin (5.0 mg/kg) treatment (Fig. 1*E*) (526,704 ± 34,261 vs. 282,586 ± 23,635 μm^2).

After 12 weeks of WD, the percentage of plaque in the total aorta, arch, thoracic, and abdominal subregions as well as the aortic sinus increased 6.4-, 7.4-, 8.5-, 4.0-, and 2.8-fold compared with standard chow–fed, vehicle-treated ApoE KO mice (Fig. 1*F–J* and representative images in Supplementary Fig. 2). Treatment with CavNOxin had no effect in standard chow–fed mice (Fig. 1*F–J*). However, in the WD-fed ApoE KO mice, CavNOxin treatment led to a 48% attenuation of total aortic plaque area as compared with vehicle-treated WD-fed ApoE KO mice (Fig. 1*F*) (lesion area: 6.80 ± 0.48 vs 3.98 ± 0.56%). The arch, thoracic, and abdominal aorta sections showed 50, 48, and 47% reduction in atherosclerosis, respectively (Fig. 1*G–I*), whereas aortic sinuses showed a 35% decrease in lesion area (Fig. 1*J*) (386,612 ± 24,044 μm^2 vs. 299 896 ± 21,607 μm^2 lesion area). These data demonstrate that CavNOxin confers a high degree of atheroprotection in STZ-induced and WD-fed ApoE KO mice.

CavNOxin Improves Endothelial Function and Decreases Oxidative Stress Markers

To confirm improvements in endothelial function in presence of atherogenic factors, WD-fed ApoE-KO mice were treated with CavNOxin or vehicle peptides for 28 days (before any major vascular morphological changes), and aortic rings were mounted on a myograph (25). PE stimulation (10^{-9}–10^{-4} mol) (Fig. 2*A*) induced concentration-dependent constriction of vehicle-treated aortas, whereas CavNOxin-treated vessels showed lower average constriction, indicative of improved endothelial function. CavNOxin-treated mice demonstrated upregulated NO function because they exhibited greater L-NAME–induced increases in PE constriction (Fig. 2*B*). In addition, plasma nitrites/nitrates, the stable oxidative products of NO, were measured. WD-fed ApoE KO mice showed plasma nitrite/nitrates levels similar to those of their standard chow–fed counterparts (Fig. 2*D*). The 12-week CavNOxin treatment led to a significant increase in plasma nitrite levels in WD-fed ApoE KO mice as compared with vehicle-treated WD-fed ApoE KO mice (Fig. 2*D*) ($P < 0.05$), indicating positive NO bioavailability upregulation. STZ induction resulted in a nonsignificant reduction of plasma nitrite levels, whereas in CavNOxin-treated STZ-induced ApoE KO mice, nitrite levels returned to that of their ND counterparts (Fig. 2*C*) (P = nonsignificant).

Because improvements in endothelial function are generally associated with decreased oxidative stress and ROS such as superoxide and peroxynitrite (35), we analyzed free radicals/hydroperoxides in the plasma as well as aortic nitrotyrosine, DHE, and 4-HNE levels, which are markers of peroxynitrite-mediated damage, superoxide, and a lipid peroxidation by-product, respectively, by immunohistochemical staining. Firstly, free radicals/hydroperoxides (dROMs test) were increased in STZ-induced ApoE KO mice and WD-fed ApoE KO mice as compared with ND and standard chow–fed mice, respectively (Fig. 2*E* and *F*) (Carratelli units). CavNOxin decreased dROMs levels in ApoE KO mice with STZ-induced diabetes at both doses (Fig. 2*E*) ($P < 0.05$). On the contrary, CavNOxin had no effect on dROMs levels in WD-fed mice (Fig. 2*F*). We observed that nitrotyrosine levels were significantly decreased by up to 56% in STZ-induced ApoE KO mice (Fig. 3*A*) and 52% in WD-fed ApoE KO mice (Fig. 3*B*) treated with CavNOxin as compared with vehicle-treated mice. Similarly, superoxide-specific DHE staining was significantly reduced by up to ~33% in STZ-induced ApoE KO mice and by 66% in WD-fed ApoE KO mice treated with CavNOxin as compared with vehicle-treated mice (Fig. 3*C* and *D*). Lastly, CavNOxin also reduced 4-HNE staining by 69% in STZ-induced ApoE KO mice, with no significant difference in WD-fed ApoE KO mice (Fig. 3 *E* and *F*). Moreover, urinary 8-isoprostane levels, a marker

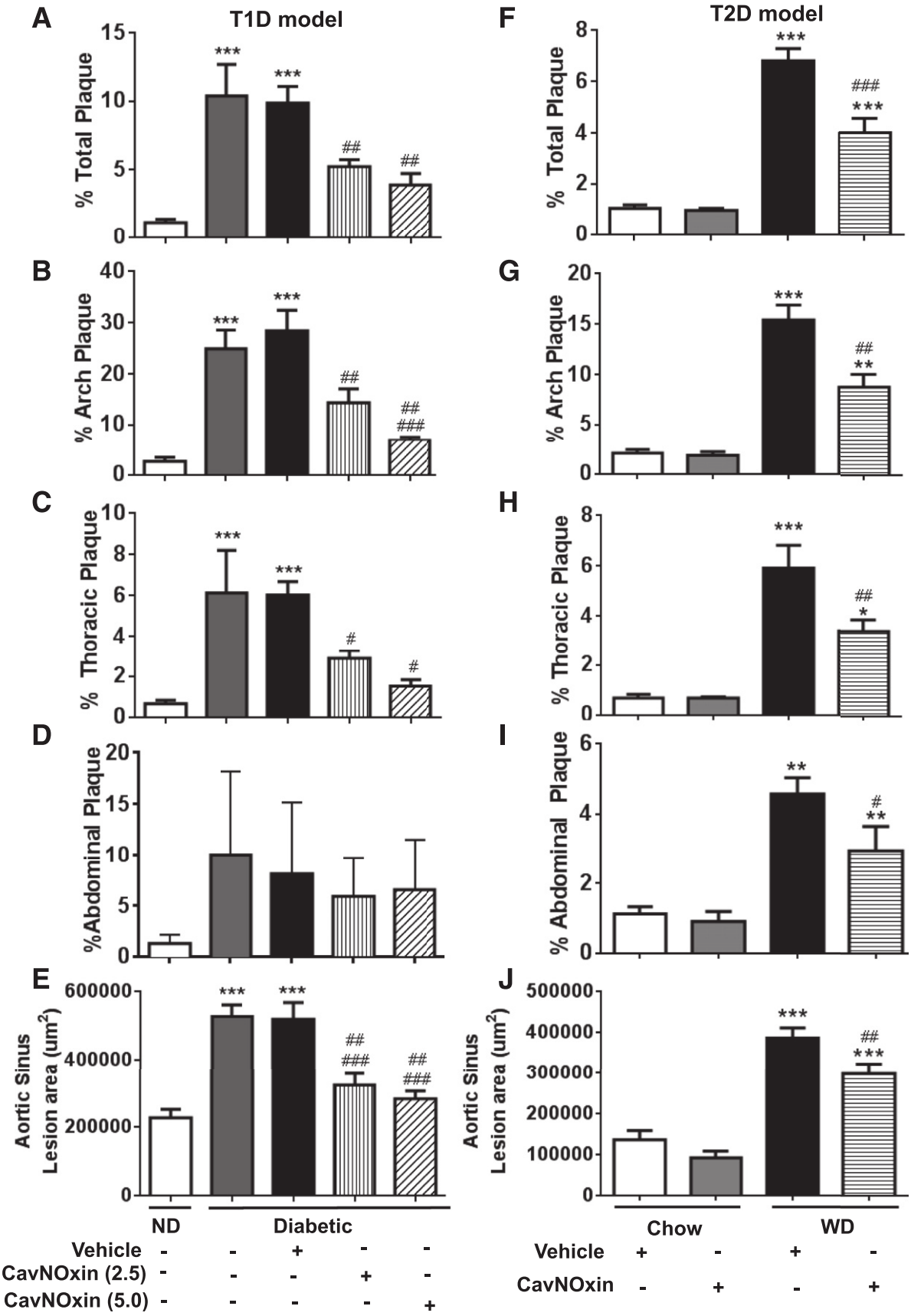

Figure 1—CavNOxin reduces atherosclerosis in STZ-induced and WD-fed ApoE KO mice. Quantification of atherosclerotic lesions in the total aorta, arch, thoracic, abdominal, and aortic sinus from ND (white), STZ-induced diabetic (gray), diabetic + vehicle (black), diabetic + CavNOxin– (2.5 mg/kg; vertical stripe), and diabetic + CavNOxin-treated (5.0 mg/kg; diagonal stripe) ApoE KO mice is shown in *A–E*,

of oxidative stress, were normalized back to ND levels in STZ-induced ApoE KO mice treated with CavNOxin (Supplementary Fig. 3*C*), whereas WD had no effect (data not shown). Finally, basal superoxide production in endothelial cells treated with vehicle or CavNOxin (1 and 5 μmol) revealed significantly reduced basal superoxide levels in CavNOxin-treated cells compared with vehicle-treated cells (Supplementary Fig. 3*D*). Taken together, these data suggest that CavNOxin confers atheroprotection through a decrease in oxidative stress.

CavNOxin Decreases the Proatherogenic Effector VCAM-1

Attenuated endothelial function is followed by endothelial activation and upregulation of adhesion molecules. Therefore, we compared the gene expression of specific proinflammatory markers listed in Supplementary Table 1 following CavNOxin treatment. From our mRNA analyses, VCAM-1, a well-known proatherogenic and proinflammatory mediator in settings of attenuated endothelial NO formation, was greatly influenced in diabetic settings and with CavNOxin treatment. In STZ-induced ApoE KO mice, the nearly threefold increase in VCAM-1 mRNA expression induced by diabetes was almost completely normalized by CavNOxin (Fig. 4*A*) and reduced by ~67% at the protein level (Fig. 4*B*). CavNOxin treatment led to a significant decrease in VCAM-1 gene expression in the aortas of WD-fed ApoE KO mice (Fig. 4*C*) (vehicle: 1.06 ± 0.17 arbitrary units [a.u.] vs. CavNOxin: 0.59 ± 0.05 a.u.) and a 64% reduction in VCAM-1 protein expression (Fig. 4*D*). In isolated endothelial cells, the VCAM-1 protein expression induced by TNF-α, a proinflammatory cytokine prominent in diabetes, was reduced by 71% with coincubation of the CavNOxin peptide (Fig. 4*E*). These data strongly suggest that CavNOxin treatment promotes a robust anti-inflammatory response, possibly as a consequence of the lowered oxidative state induced by CavNOxin. This anti-inflammatory effect of the peptide is further supported by significant reductions in staining for a macrophage marker, F4/80, as well as reductions in MCP-1 gene expression in STZ-induced ApoE KO aortas (Supplementary Fig. 3*A* and *B*).

CavNOxin Decreases Monocyte-Endothelial Interactions In Vitro

Because attenuated VCAM-1 levels with CavNOxin treatment should translate into decreased leukocyte–endothelial cell interactions, cultured HAECs were pretreated for 6 h with CavNOxin (5 μmol), which led to a 39% decrease in the adhesion of human monocytic THP-1 cells in static adhesion assays (Fig. 5*A*). Under high glucose (30 mmol) conditions for 3 days, an increase in THP-1 cell adhesion was observed (Fig. 5*B*) when compared with low-glucose (5 mmol) treatment, whereas CavNOxin treatment completely blocked THP-1 cell adhesion as a result of high glucose (Fig. 5*B*).

CavNOxin Decreases Dynamic Aortic Vascular Adhesion Ex Vivo

To confirm the in vitro effects of CavNOxin on leukocyte–endothelial adhesion, we examined the adhesion of human leukocytes to isolated aortas. Under basal conditions, there were no observed differences in the number of adherent leukocytes between ApoE KO aortas treated with the vehicle or CavNOxin peptides (Fig. 5*C* and *D*). TNF-α (5 ng/mL; 4 h) induced a significant time-dependent increase in the number of adhered leukocytes after 10 and 15 min (Fig. 5*C* and *D*), which was almost completely abolished in aortas coincubated with CavNOxin (Fig. 5*C* and *D*) (vehicle + TNF: 16 ± 3 cells vs. CavNOxin + TNF: 8 ± 2 cells after 15 min). Similarly, diabetic aortas showed higher numbers of adherent leukocytes (Fig. 5*E* and *F*) (diabetic vs. ND), whereas, importantly, diabetes-induced adhesion was completely blocked by CavNOxin treatment (Fig. 5*E* and *F*) (diabetic: 15 ± 2 cells vs. CavNOxin 5 ± 2 cells after 15 min). Our in vitro and ex vivo data demonstrate that CavNOxin blocks leukocyte–endothelial interactions, a key step in early atherogenesis.

ApoE KO Mice Lacking eNOS Gene Are Resistant to CavNOxin Treatment

To confirm that CavNOxin mediates its therapeutic effect through eNOS, we generated ApoE/eNOS dKO mice. When fed a WD, these mice showed threefold increase in atherosclerotic burden compared with ApoE KO mice fed the same WD (ApoE KO: 6.8% total plaque [see Fig. 1*A*] vs. ApoE/eNOS dKO: 18% total plaque [Fig. 6*B*]). Interestingly, treatment with either vehicle or CavNOxin peptide (Fig. 6*A–E*) resulted in similar atherosclerotic lesions in WD ApoE/eNOS dKO and similar nitrotyrosine staining (Fig. 6*F*). This lack of effect of the CavNOxin peptide on atherosclerotic lesions in the ApoE/eNOS dKO mice is constant with a high degree of specificity of the CavNOxin peptide for eNOS and indicates that CavNOxin likely decreases eNOS-derived oxidative stress in addition to increasing eNOS-derived NO, resulting in atheroprotection.

DISCUSSION

Our study exhibits for the first time in vivo, in two experimental models of diabetes, namely, the STZ-induced T1D model and the T2D WD-induced insulin-resistant

respectively. ***$P < 0.001$ vs. ND group, #$P < 0.05$, ##$P < 0.01$ vs. diabetic and diabetic + vehicle group, ###$P < 0.001$ vs. diabetic + vehicle group. Quantification of atherosclerotic lesions in the total aorta, arch, thoracic, abdominal, and aortic sinus from chow-fed + vehicle-treated (white), chow-fed + CavNOxin-treated (gray), WD-fed + vehicle-treated (black), and WD-fed + CavNOxin-treated (horizontal stripe) ApoE KO mice is shown in *F–J*, respectively. *$P < 0.05$, **$P < 0.01$, ***$P < 0.001$ vs. chow + vehicle; #$P < 0.05$, ##$P < 0.01$, ###$P < 0.001$ vs. WD + vehicle. n = 5–10/group (for *A–E*) and n = 10/group (for *F–J*). All results expressed as mean ± SEM.

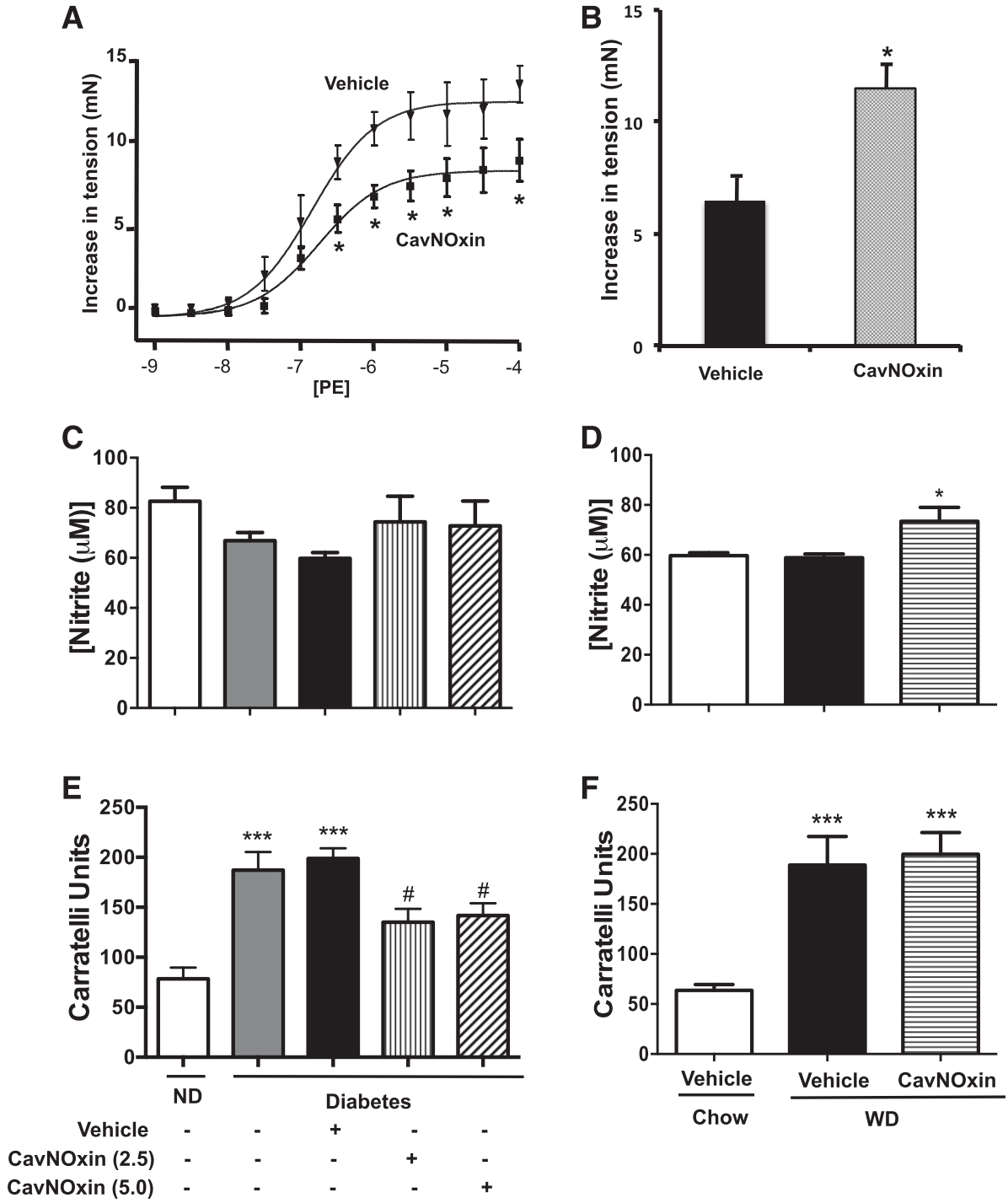

Figure 2—CavNOxin increases endothelial function and attenuates oxidative stress in vivo. *A* and *B*: CavNOxin-treated aortas from WD-fed ApoE KO mice show decreased PE-induced constrictions (mN) (squares) when compared with vehicle-treated aortas (triangle). *B*: Average increase in constriction induced by L-NAME (10^{-6} mol). $n = 4$/group. $^{*}P < 0.05$. Total plasma nitrite concentration is shown for ApoE KO mice with STZ-induced diabetes (*C*) and for WD-fed ApoE KO mice (*D*) treated with vehicle or CavNOxin. $^{*}P < 0.05$ vs. chow + vehicle. dROMs analysis is shown in ApoE KO mice with STZ-induced diabetes (*E*) and WD-fed ApoE KO mice (*F*) treated with vehicle or CavNOxin. For *C* and *E*, bars represent ND (white), STZ-induced diabetic (gray), diabetic + vehicle treatment (black), diabetic + CavNOxin (2.5 mg/kg) (vertical stripe), and diabetic + CavNOxin (5.0 mg/kg) (diagonal stripe) ApoE KO mice. $^{***}P < 0.01$ vs. or ND for chow (*E*) + vehicle for *F*, $\#P < 0.05$ vs. diabetic and diabetic + vehicle. $n = 7$–10/group (for *C* and *E*) and $n = 10$/group (for *D* and *F*). All results expressed as mean ± SEM.

model, that relieving eNOS from the inhibitory clamp of Cav-1 leads to the marked attenuation of atherosclerosis. It is generally well accepted that endothelial dysfunction with its accompanying reduced NO bioavailability contributes to early atherogenesis in diabetes, predominantly by modulating oxidative stress and leukocyte–endothelial

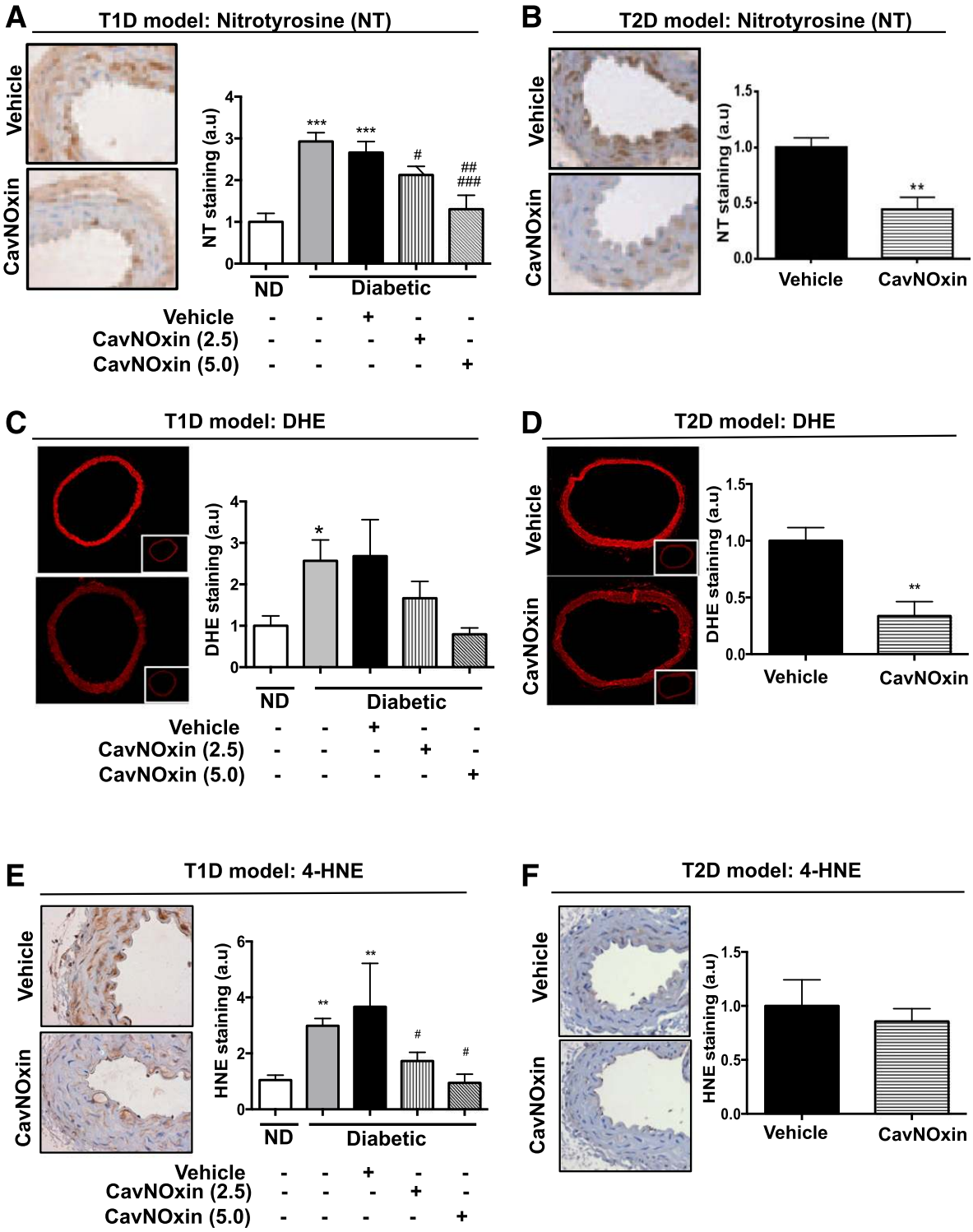

Figure 3—CavNOxin reduces oxidative stress parameters. Representative images and quantification of aortas stained with anti-NT antibody from ApoE KO mice with STZ-induced diabetes (*A*) and WD-fed ApoE KO mice (*B*) treated with vehicle or CavNOxin. ***$P <$ 0.001 vs. ND group, #$P < 0.05$ vs. diabetic + vehicle group, ###$P < 0.001$ vs. diabetic group for *A*; **$P < 0.01$ vs. WD + vehicle group for *B*. Representative images and quantification of superoxide detection by fluorescence imaging of DHE and DHE plus tempol (inset) in aortas of STZ-induced diabetic (*C*) and WD-fed ApoE KO mice (*D*) treated with vehicle or CavNOxin. *$P < 0.05$ vs. ND for *C*. **$P < 0.01$ vs. WD + vehicle for *D*. Representative images and quantification of aortas stained with 4-HNE from STZ-induced diabetic (*E*) and WD-fed ApoE KO mice (*F*) treated with vehicle or CavNOxin. **$P < 0.01$ vs. ND group, #$P < 0.05$ vs. diabetic and diabetic + vehicle group. For *A*, *C*, and *E*, bars represent ND (white), STZ-induced diabetic (gray), diabetic + vehicle treatment (black), diabetic + CavNOxin (2.5 mg/kg) (vertical stripe), and diabetic + CavNOxin (5.0 mg/kg) (diagonal stripe) ApoE KO mice. n = 5–10/group. All results expressed as mean ± SEM.

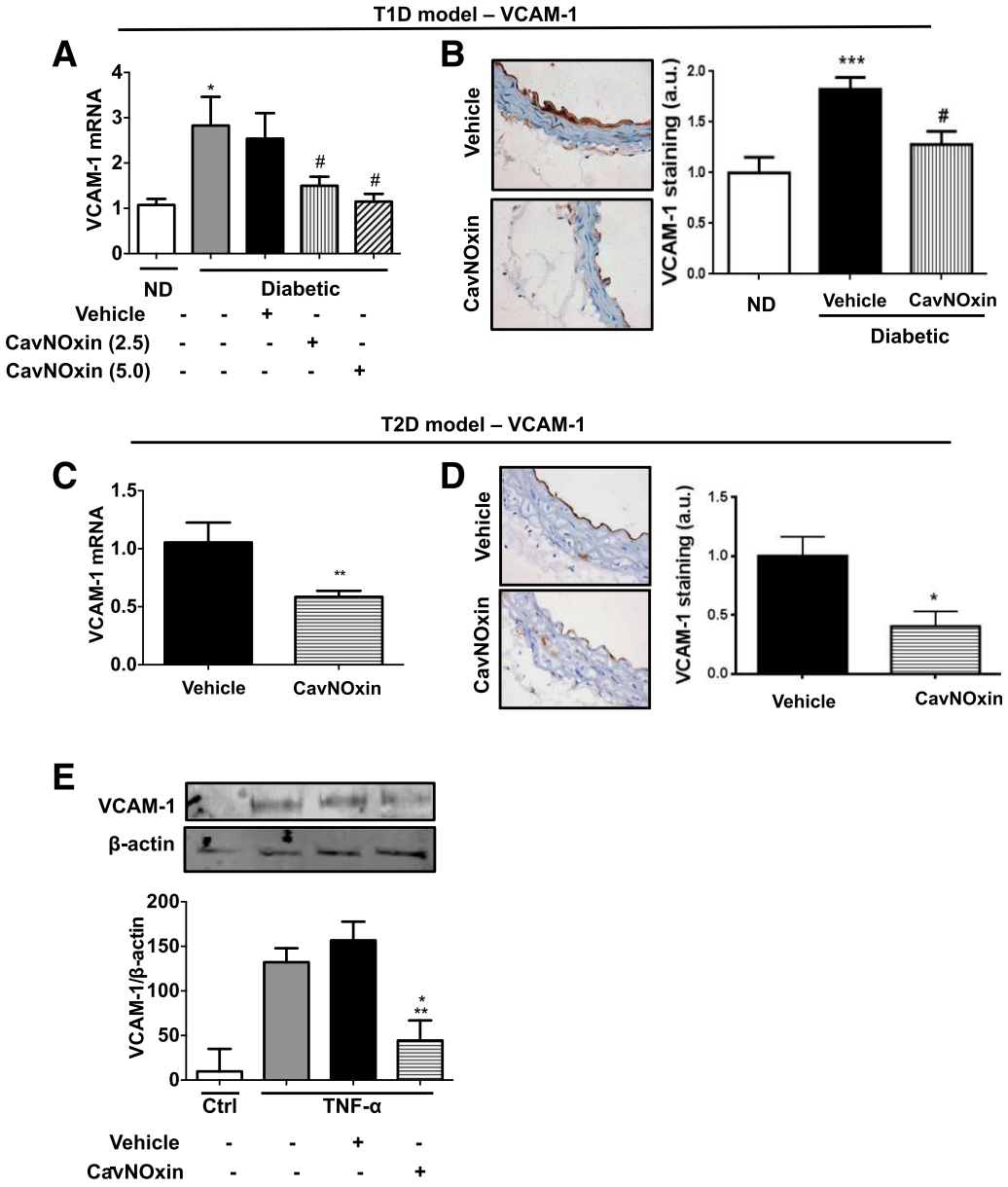

Figure 4—CavNOxin decreases VCAM-1 expression in ApoE KO mice with STZ-induced diabetes and WD-fed ApoE KO mice. *A*: VCAM-1 mRNA expression levels determined by qRT-PCR and expressed as fold induction relative to ND controls. Bars represent ND (white), STZ-induced diabetic (gray), diabetic + vehicle treatment (black), diabetic + CavNOxin (vertical stripe), and diabetic + CavNOxin (5.0 mg/kg) (diagonal stripe) ApoE KO mice. *B*: Representative images and quantification of VCAM-1 immunostaining in aortas of STZ-induced diabetic ApoE KO mice treated with vehicle or CavNOxin (combined value for both 2.5 and 5.0 mg/kg doses). $^{*}P < 0.05$, $^{***}P < 0.001$ vs. ND group, #$P <$ 0.05 vs. diabetic. *C*: VCAM-1 mRNA expression levels determined by qRT-PCR and expressed as fold induction relative to vehicle controls in WD-fed ApoE KO mice. *D*: Representative images and quantification of VCAM-1 immunostaining in aortas of WD-fed ApoE KO mice treated with vehicle or CavNOxin. $^{*}P < 0.05$, $^{**}P < 0.01$ vs. vehicle group. *E*: Western blot and densitometry of VCAM-1 protein expression relative to β-actin in HAECs treated with either vehicle or CavNOxin peptide (5 μmol for 6 h) in the presence of TNF-α (0.5 ng/ml). $^{*}P < 0.05$ vs. TNF-α–treated group, $^{**}P < 0.01$ vs. vehicle + TNF-α–treated group. n = 5–10/group. Bars represent control (white), TNF-α–treated (gray), TNF-α + vehicle–treated (black), and TNF-α + CavNOxin–treated (horizontal stripe) endothelial cells. All results expressed as mean ± SEM. Ctrl, control.

interactions. Through the use of CavNOxin, a cell-permeable Cav-1 peptide with an inactivated eNOS inhibitory domain, we demonstrate that increasing endogenous eNOS-derived NO release attenuated diabetes-induced atherosclerotic plaque, which correlated with reductions in oxidative stress markers, a decrease in proinflammatory mediators, and a lessening of leukocyte adherence to the vascular endothelium. Furthermore, CavNOxin had no effect on atherosclerosis in the ApoE/eNOS dKO mouse, confirming the specificity of our eNOS-activating approach—a key finding because NO is also produced by neuronal NOS and inducible NO and the expression of

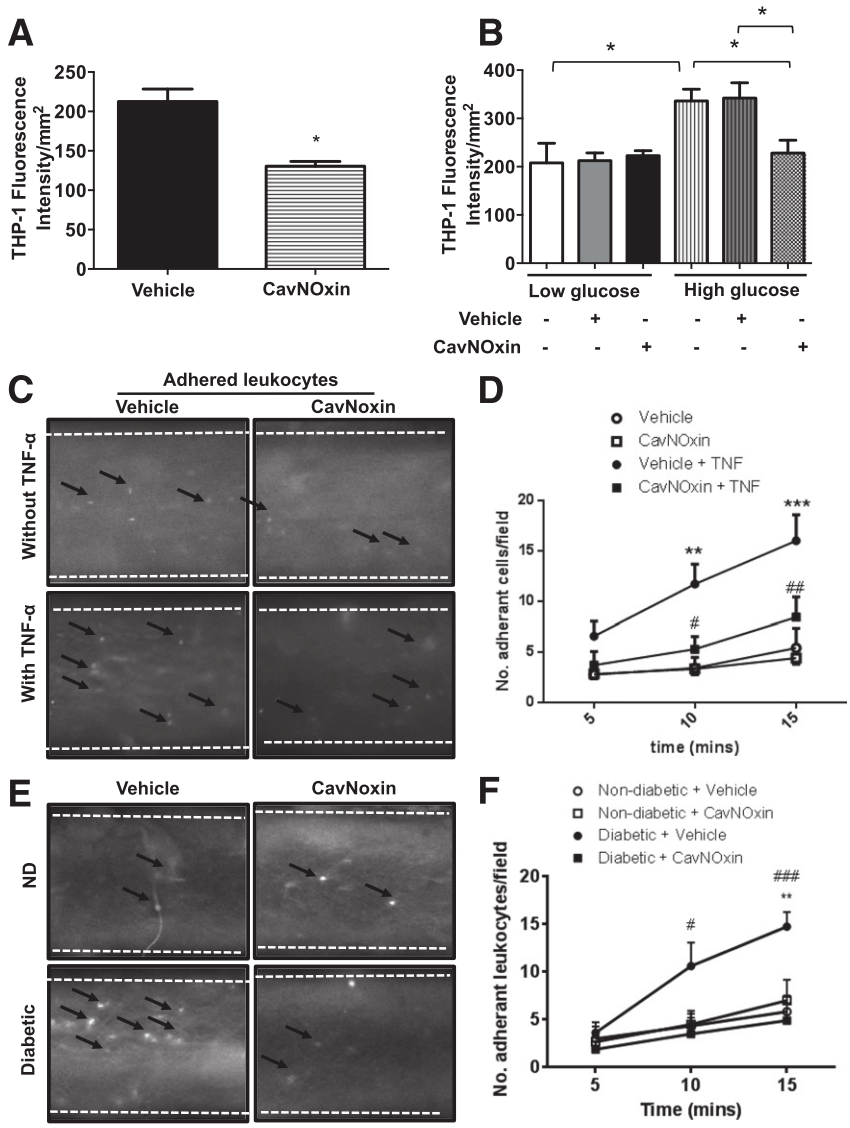

Figure 5—CavNOxin reduces monocyte–endothelial cell interactions in vitro and ex vivo. *A*: Quantification of adherent human THP-1 monocytic cells to HAECs treated with vehicle or CavNOxin peptide. *$P < 0.05$ vs. vehicle group. *B*: Quantification of adherent THP-1 cells to HAECs grown in either low glucose (5 mmol) or high glucose (30 mmol) and treated with vehicle or CavNOxin peptide. *$P < 0.05$ as indicated. Bars represent low glucose (LG) (white), LG + vehicle–treated (gray), LG + CavNOxin–treated (black), high glucose (HG) (vertical stripe), HG + vehicle–treated (gray vertical stripe), and HG + CavNOxin–treated (gray pattern) endothelial cells. *C*: Representative images showing leukocytes (arrows) binding to the aortic surface at the 15-min time point after TNF-α stimulation. *D*: Quantitation of average leukocyte binding per field every 5 min over a 15-min period. **$P < 0.05$, ***$P < 0.001$ vs. vehicle group, #$P < 0.05$, ##$P < 0.01$ vs. vehicle + TNF-α–treated group. *E*: Representative images showing leukocytes (arrows) binding to the aortic surface of diabetic and ND aortas at the 15-min time point. *F*: Quantitation of average leukocyte binding per field every 5 min over a 15-min period. **$P < 0.01$ vs ND + vehicle group. #$P < 0.05$, ###$P < 0.01$ vs. diabetic + CavNOxin–treated group. n = 6–8/group. All results expressed as mean ± SEM.

both of these isoforms has been shown to be upregulated in advanced atherosclerotic plaques (18).

Bioavailability of NO is critically dependent on the delicate balance between eNOS-derived NO synthesis and superoxide inactivation of NO, with the balance tipping in favor of the latter in the diabetic setting. Therefore, limiting ROS production is an important therapeutic avenue in promoting NO bioavailability. In our study, systemic oxidative stress and ROS-related tissue damage was detected in both models, which correlated with the increase in atherosclerotic burden. This observation is confirmed in human studies, which show high levels of a specific lipid peroxidase biomarker, reflecting oxidative stress in the diabetic population (36). Recent studies have uncovered that the predominant source of ROS in diabetic macrovascular disease includes uncoupled eNOS. Indeed, eNOS uncoupling is so profound in the diabetic endothelium that eNOS-derived superoxide causes augmentation of vascular remodeling and dysfunction, strengthening the notion that proper regulation of eNOS is required to protect against atherosclerosis, particularly in the diabetic milieu (37). In this study, we demonstrated a novel

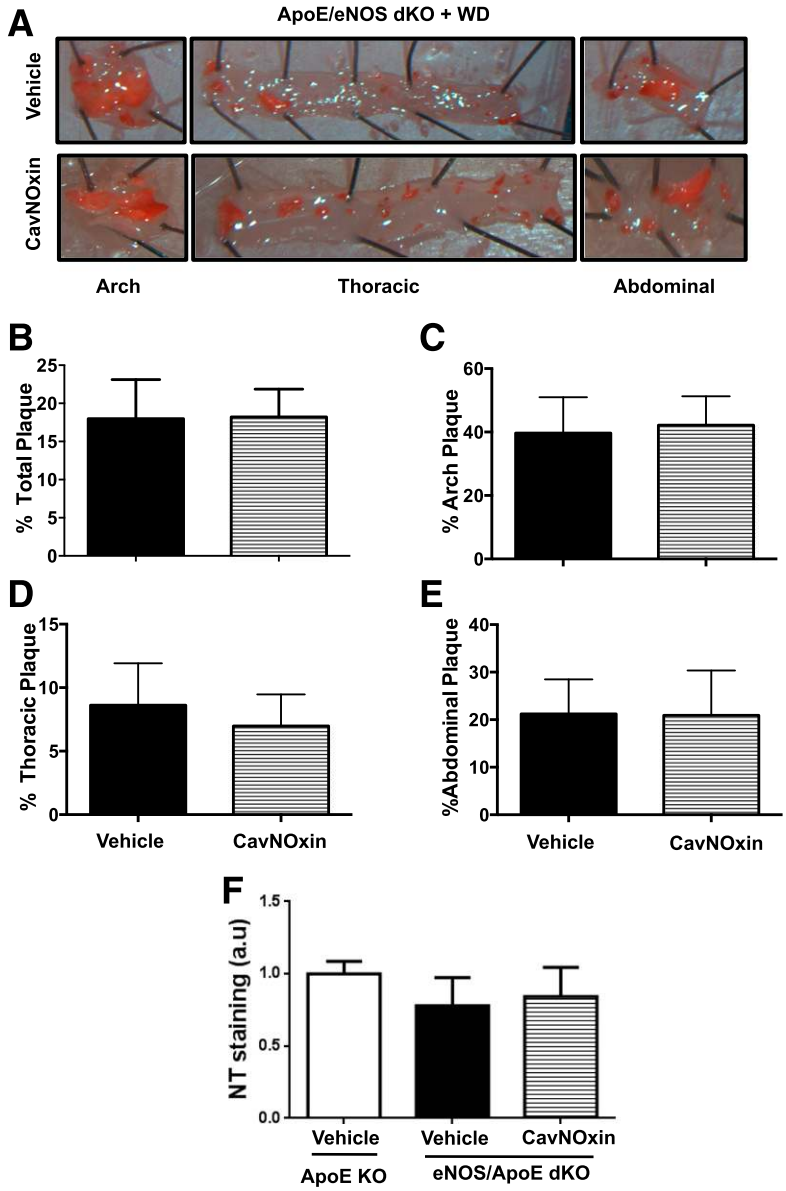

Figure 6—CavNOxin does not have an antiatherosclerotic effect in eNOS/ApoE dKO mice. *A*: Sudan IV–stained aortas from WD-fed eNOS/ApoE dKO mice treated with vehicle or CavNOxin peptides. Percent total plaque area in the aorta, percent arch plaque area, percent thoracic plaque area, and percent abdominal plaque area are shown in *B–E*, respectively. *F*: Quantification of aortas stained with anti-NT antibody from WD-fed ApoE KO mice and WD-fed eNOS/ApoE dKO mice treated with vehicle or CavNOxin. n = 5 to 6/group. All results are expressed as mean ± SEM.

antioxidant effect of CavNOxin, as it was able to significantly decrease systemic oxidative stress as well as vascular tissue damage induced by peroxynitrite and lipid peroxidation. We postulate that the decrease in oxidative stress observed in this study is a result of CavNOxin's effect on eNOS signaling, as reflected by the failure of CavNOxin to confer antiatherosclerotic effects in ApoE/eNOS dKO mice.

A central mechanism driving diabetes-associated vascular diseases is inflammation, which triggers endothelial dysfunction and enhances the proadhesive and prothrombotic properties of the endothelium, thereby promoting the recruitment of inflammatory cells to the vascular wall. Another key finding of our work stems from the observation that CavNOxin-induced NO upregulation was able to attenuate aortic and endothelial VCAM-1 expression, which correlated closely with the reduction in leukocyte/monocyte adhesion to the vascular wall and to cultured endothelial cells in diabetic and inflammatory (TNF-α) settings, lending credence to previous studies that demonstrated decreased leukocyte recruitment and VCAM-1 expression in Cav-1 KO tissues (38–40). Furthermore, increased eNOS activity has been associated with the downregulation of adhesion molecules, in particular VCAM-1 (19), and our data suggest that this can be achieved specifically through endogenous eNOS in a compensatory manner because hyperglycemia is a potent

inducer of leukocyte–endothelial interactions (13,41). In addition, oxidative stress is known to regulate proinflammatory mediators such as VCAM-1 (42). Given the positive effects of CavNOxin in lowering superoxide, it is feasible that the dampening of VCAM-1 levels occurs in response to the CavNOxin-driven lowered oxidative stress. It is also possible that CavNOxin mediates its anti-inflammatory effects on VCAM-1 through modifications of blood flow, which are known to affect VCAM-1 levels (43).

Although decreased eNOS-derived NO bioavailability has long been linked to an increased incidence and severity of cardiovascular disease, whether endogenous eNOS-derived NO release can be stimulated specifically to promote atheroprotection is unknown. As outlined previously, the potential action of promoting eNOS bioavailability may indeed be particularly relevant in diabetes, which is a state of NO deficiency. A few studies have documented the feasibility of increasing eNOS-derived NO release by decreasing the eNOS interaction with Cav-1 (44–47). However, these previous studies were performed using no NOS-specific pharmacological agents, such as HMGCoA reductase inhibitors (statins) or a smooth muscle cell Ca^{2+} channel blocker (amlodipine) in nonatherogenic or diabetic settings. Cardiovascular drugs such as statins, ACE inhibitors, angiotensin receptor blockers, β-blockers, (reviewed in 48), or BH_4 supplementation (49) can increase NO release in clinical or preclinical settings, but these are pleiotropic or secondary effects rather than direct modulation of eNOS-derived NO. The high degree of CavNOxin specificity toward eNOS allows us to postulate that within diseased vessels, there exists an atheroprotective, eNOS-derived endothelial reserve function despite the presence of endothelial dysfunction-inducing atherogenic factors. Our data have therefore shown that directly improving endothelial function through specific targeting of eNOS via an eNOS/Cav-1–dependent mechanism results in atheroprotection in diabetes-induced atherosclerosis. More importantly, the unique ability of CavNOxin to regulate eNOS activity while preserving caveolae/Cav-1 biology makes it a desirable therapeutic agent. However, further validation in models of T1D and T2D is now warranted, particularly those in whom dyslipidemia may not play such a prominent role, for example, the STZ-induced LDL-$R^{-/-}$ mouse (for T1D) or the db/db model of T2D. In addition, our data suggest that the potential targeting of this site, via either novel agonistic peptides or small molecules, holds promise as a targeted antiatherogenic therapy under conditions of high glucose and elevated lipids as seen in patients with diabetes.

Acknowledgments. The authors thank the Vascular Pharmacology Laboratory of Professor Jaye Chin-Dusting at the Baker IDI Heart and Diabetes Institute (Melbourne) for allowing the use of equipment for the flow adhesion studies and Irene Carmichael of Monash Micro Imaging from Alfred Medical Research and Education Precinct (Melbourne) for assistance with DHE imaging.

Funding. J.B.d.H. was supported by Australian National Health and Medical Research Council grant 1005851. P.B. is supported by grants from the Canadian Institutes of Health Research, Heart and Stroke Foundation of Canada, Heart and Stroke Foundation of BC and Yukon, Michael Smith Foundation for Health Research, Canadian Foundation for Innovation, and British Columbia Knowledge Development Foundation. A.S. is supported by the Alexander Graham Bell Canada Graduate Scholarship, Four Year Doctoral Fellowship from Canadian Institutes of Health Research/University of British Columbia, and the Baker IDI Top-up Scholarship. This work was supported in part by the Victorian Government's Operational Infrastructure Support Program.

Duality of Interest. No potential conflicts of interest relevant to this article were reported.

Author Contributions. A.S. researched data, developed the study design, and wrote the manuscript. S.S., N.S., C.L., S.M.T., and O.H. researched data. D.J.G. reviewed and edited the manuscript. M.E.C. contributed to discussion and reviewed the edited manuscript. J.B.d.H. and P.B. developed the study design and reviewed the edited manuscript. A.S. is the guarantor of this work and, as such, had full access to all the data in the study and takes responsibility for the integrity of the data and the accuracy of the data analysis.

References

1. Funk SD, Yurdagul A Jr, Orr AW. Hyperglycemia and endothelial dysfunction in atherosclerosis: lessons from type 1 diabetes. Int J Vasc Med 2012;2012:569654
2. Pyörälä K, Laakso M, Uusitupa M. Diabetes and atherosclerosis: an epidemiologic view. Diabetes Metab Rev 1987;3:463–524
3. Sharma A, Bernatchez PN, de Haan JB. Targeting endothelial dysfunction in vascular complications associated with diabetes. Int J Vasc Med 2012;2012:750126
4. Mannucci E, Dicembrini I, Lauria A, Pozzilli P. Is glucose control important for prevention of cardiovascular disease in diabetes? Diabetes Care 2013; 36(Suppl. 2):S259–S263
5. Kolka CM, Bergman RN. The endothelium in diabetes: its role in insulin access and diabetic complications. Rev Endocr Metab Disord 2013;14:13–19
6. Chigaev A, Smagley Y, Sklar LA. Nitric oxide/cGMP pathway signaling actively down-regulates α4β1-integrin affinity: an unexpected mechanism for inducing cell de-adhesion. BMC Immunol 2011;12:28
7. De Caterina R, Libby P, Peng HB, et al. Nitric oxide decreases cytokine-induced endothelial activation. Nitric oxide selectively reduces endothelial expression of adhesion molecules and proinflammatory cytokines. J Clin Invest 1995;96:60–68
8. Roberts W, Riba R, Homer-Vanniasinkam S, Farndale RW, Naseem KM. Nitric oxide specifically inhibits integrin-mediated platelet adhesion and spreading on collagen. J Thromb Haemost 2008;6:2175–2185
9. Carantoni M, Abbasi F, Chu L, et al. Adherence of mononuclear cells to endothelium in vitro is increased in patients with NIDDM. Diabetes Care 1997;20: 1462–1465
10. Clarkson P, Celermajer DS, Donald AE, et al. Impaired vascular reactivity in insulin-dependent diabetes mellitus is related to disease duration and low density lipoprotein cholesterol levels. J Am Coll Cardiol 1996;28:573–579
11. Ding H, Triggle CR. Endothelial cell dysfunction and the vascular complications associated with type 2 diabetes: assessing the health of the endothelium. Vasc Health Risk Manag 2005;1:55–71
12. McVeigh GE, Brennan GM, Johnston GD, et al. Impaired endothelium-dependent and independent vasodilation in patients with type 2 (non-insulin-dependent) diabetes mellitus. Diabetologia 1992;35:771–776
13. Morigi M, Angioletti S, Imberti B, et al. Leukocyte-endothelial interaction is augmented by high glucose concentrations and hyperglycemia in a NF-kB-dependent fashion. J Clin Invest 1998;101:1905–1915
14. Srinivasan S, Hatley ME, Bolick DT, et al. Hyperglycaemia-induced superoxide production decreases eNOS expression via AP-1 activation in aortic endothelial cells. Diabetologia 2004;47:1727–1734
15. Salt IP, Morrow VA, Brandie FM, Connell JM, Petrie JR. High glucose inhibits insulin-stimulated nitric oxide production without reducing endothelial nitric-oxide synthase Ser1177 phosphorylation in human aortic endothelial cells. J Biol Chem 2003;278:18791–18797
16. Kuhlencordt PJ, Gyurko R, Han F, et al. Accelerated atherosclerosis, aortic aneurysm formation, and ischemic heart disease in apolipoprotein E/endothelial nitric oxide synthase double-knockout mice. Circulation 2001;104:448–454

17. Cayatte AJ, Palacino JJ, Horten K, Cohen RA. Chronic inhibition of nitric oxide production accelerates neointima formation and impairs endothelial function in hypercholesterolemic rabbits. Arterioscler Thromb 1994;14:753–759
18. Wilcox JN, Subramanian RR, Sundell CL, et al. Expression of multiple isoforms of nitric oxide synthase in normal and atherosclerotic vessels. Arterioscler Thromb Vasc Biol 1997;17:2479–2488
19. Ozaki M, Kawashima S, Yamashita T, et al. Overexpression of endothelial nitric oxide synthase accelerates atherosclerotic lesion formation in apoE-deficient mice. J Clin Invest 2002;110:331–340
20. Liu J, García-Cardeña G, Sessa WC. Palmitoylation of endothelial nitric oxide synthase is necessary for optimal stimulated release of nitric oxide: implications for caveolae localization. Biochemistry 1996;35:13277–13281
21. Bernatchez PN, Bauer PM, Yu J, Prendergast JS, He P, Sessa WC. Dissecting the molecular control of endothelial NO synthase by caveolin-1 using cell-permeable peptides. Proc Natl Acad Sci U S A 2005;102:761–766
22. Bucci M, Gratton JP, Rudic RD, et al. In vivo delivery of the caveolin-1 scaffolding domain inhibits nitric oxide synthesis and reduces inflammation. Nat Med 2000;6:1362–1367
23. García-Cardeña G, Martasek P, Masters BS, et al. Dissecting the interaction between nitric oxide synthase (NOS) and caveolin. Functional significance of the nos caveolin binding domain in vivo. J Biol Chem 1997;272:25437–25440
24. Gratton JP, Lin MI, Yu J, et al. Selective inhibition of tumor microvascular permeability by cavtratin blocks tumor progression in mice. Cancer Cell 2003;4:31–39
25. Bernatchez P, Sharma A, Bauer PM, Marin E, Sessa WC. A noninhibitory mutant of the caveolin-1 scaffolding domain enhances eNOS-derived NO synthesis and vasodilation in mice. J Clin Invest 2011;121:3747–3755
26. Trane AE, Pavlov D, Sharma A, et al. Deciphering the binding of caveolin-1 to client protein endothelial nitric-oxide synthase (eNOS): scaffolding subdomain identification, interaction modeling, and biological significance. J Biol Chem 2014;289:13273–13283
27. de Haan JB, Witting PK, Stefanovic N, et al. Lack of the antioxidant glutathione peroxidase-1 does not increase atherosclerosis in C57BL/J6 mice fed a high-fat diet. J Lipid Res 2006;47:1157–1167
28. Winzell MS, Ahrén B. The high-fat diet-fed mouse: a model for studying mechanisms and treatment of impaired glucose tolerance and type 2 diabetes. Diabetes 2004;53(Suppl. 3):S215–S219
29. Wu KK, Huan Y. Diabetic atherosclerosis mouse models. Atherosclerosis 2007;191:241–249
30. Phillips JW, Barringhaus KG, Sanders JM, et al. Rosiglitazone reduces the accelerated neointima formation after arterial injury in a mouse injury model of type 2 diabetes. Circulation 2003;108:1994–1999
31. Chew P, Yuen DY, Koh P, et al. Site-specific antiatherogenic effect of the antioxidant ebselen in the diabetic apolipoprotein E-deficient mouse. Arterioscler Thromb Vasc Biol 2009;29:823–830
32. Lewis P, Stefanovic N, Pete J, et al. Lack of the antioxidant enzyme glutathione peroxidase-1 accelerates atherosclerosis in diabetic apolipoprotein E-deficient mice. Circulation 2007;115:2178–2187
33. Chew P, Yuen DY, Stefanovic N, et al. Antiatherosclerotic and renoprotective effects of ebselen in the diabetic apolipoprotein E/GPx1-double knockout mouse. Diabetes 2010;59:3198–3207
34. Tikellis C, Pickering RJ, Tsorotes D, et al. Activation of the Renin-Angiotensin system mediates the effects of dietary salt intake on atherogenesis in the apolipoprotein E knockout mouse. Hypertension 2012;60:98–105
35. Förstermann U, Li H. Therapeutic effect of enhancing endothelial nitric oxide synthase (eNOS) expression and preventing eNOS uncoupling. Br J Pharmacol 2011;164:213–223
36. Szuchman A, Aviram M, Musa R, Khatib S, Vaya J. Characterization of oxidative stress in blood from diabetic vs. hypercholesterolaemic patients, using a novel synthesized marker. Biomarkers 2008;13:119–131
37. Bonomini F, Tengattini S, Fabiano A, Bianchi R, Rezzani R. Atherosclerosis and oxidative stress. Histol Histopathol 2008;23:381–390
38. Fernández-Hernando C, Yu J, Suárez Y, et al. Genetic evidence supporting a critical role of endothelial caveolin-1 during the progression of atherosclerosis. Cell Metab 2009;10:48–54
39. Fernández-Hernando C, Yu J, Dávalos A, Prendergast J, Sessa WC. Endothelial-specific overexpression of caveolin-1 accelerates atherosclerosis in apolipoprotein E-deficient mice. Am J Pathol 2010;177:998–1003
40. Engel D, Beckers L, Wijnands E, et al. Caveolin-1 deficiency decreases atherosclerosis by hampering leukocyte influx into the arterial wall and generating a regulatory T-cell response. FASEB J 2011;25:3838–3848
41. Kim JA, Berliner JA, Natarajan RD, Nadler JL. Evidence that glucose increases monocyte binding to human aortic endothelial cells. Diabetes 1994;43:1103–1107
42. Marui N, Offermann MK, Swerlick R, et al. Vascular cell adhesion molecule-1 (VCAM-1) gene transcription and expression are regulated through an antioxidant-sensitive mechanism in human vascular endothelial cells. J Clin Invest 1993;92:1866–1874
43. Nakashima Y, Raines EW, Plump AS, Breslow JL, Ross R. Upregulation of VCAM-1 and ICAM-1 at atherosclerosis-prone sites on the endothelium in the ApoE-deficient mouse. Arterioscler Thromb Vasc Biol 1998;18:842–851
44. Feron O, Dessy C, Desager JP, Balligand JL. Hydroxy-methylglutaryl-coenzyme A reductase inhibition promotes endothelial nitric oxide synthase activation through a decrease in caveolin abundance. Circulation 2001;103:113–118
45. Sharma A, Trane A, Yu C, Jasmin JF, Bernatchez P. Amlodipine increases endothelial nitric oxide release by modulating binding of native eNOS protein complex to caveolin-1. Eur J Pharmacol 2011;659:206–212
46. Zhou Q, Liao JK. Pleiotropic effects of statins. - Basic research and clinical perspectives -. Circ J 2010;74:818–826
47. Liao JK, Laufs U. Pleiotropic effects of statins. Annu Rev Pharmacol Toxicol 2005;45:89–118
48. Mordi I, Tzemos N. Is reversal of endothelial dysfunction still an attractive target in modern cardiology? World J Cardiol 2014;6:824–835
49. Christ SE, Moffitt AJ, Peck D, White DA. The effects of tetrahydrobiopterin (BH4) treatment on brain function in individuals with phenylketonuria. Neuroimage Clin 2013;3:539–547